Undersampling to Regularize the Source Reconstruction Problem for an Electric Point Source

S. G. Sen
Electrical Electronics Engineering Department, Ataturk University, Turkey

Abstract— In this article, a source reconstruction problem is solved by sampling the tangential components of the electric field of an electric point source on the surface of a hemisphere the center of which is the location of the point source. The source reconstruction is performed by sampling the electric field at five different sampling rates. One of the sampling rate corresponds to the Nyquist rate, two of them are oversampling rates and the rest are undersampling rates. The problem is discretized into a matrix equation which is solved iteratively. For each of the solution iterate, the field components are reconstructed and the error with respect to the original fields are computed. It is shown that the error made is approximately the same for all the sampling rates. In addition, the fields are reconstructed on hemispheres outside the sampling hemisphere. The error made in this reconstruction is calculated and shown to be not too much varying among the five different sampling rates. By means of these two field reconstruction demonstrations, it is proven that the oversampling and Nyquist rate sampling do in fact provide redundant information for the source reconstruction since the oversampling and the Nyquist rate sampling do not increase the accuracy of the reconstructed fields. The current reconstruction is also made using the lowest sampling rate and it is indicated that the reconstructed current is close to the original current although the sampling rate is lowest. As a result, it is determined that undersampling regularizes the reconstruction problem by deleting the redundant information due to higher rate sampling.

1. INTRODUCTION

It is possible to determine the radiation pattern of an antenna using the antenna material properties and the antenna geometry as inputs to the electromagnetic analysis. However, the electromagnetic analysis can never produce the actual radiation properties of the manufactured antenna because the defects in the manufacturing material, distortions in the geometry of the antenna, cables and supporting accessories around the antenna cause deviations from the theoretical antenna radiation pattern. All of these real life effects can be taken into consideration by the source reconstruction method and the actual antenna radiation pattern can be determined [1].

In the source reconstruction method, the field of the actual source is sampled to obtain the necessary information for the reconstruction of the original source. The relation between the source and its fields expressed using the mixed potential integral equation is not a Fourier transform relation as indicated in [2]. Hence, it is possible to reduce the field sampling rate below the Nyquist sampling rate. In this article, the electric field components which are tangential to a hemisphere centered at the point source of the electric field ($\vec{E}$) are sampled and from these samples, the point source is reconstructed. Three sampling rates are employed: Oversampling, Nyquist rate sampling and undersampling. These sampling rates are compared according to the reconstructed field accuracy and the speed of convergence to the reconstructed source solution. The comparison shows that three different sampling schemes do not yield results very much differing from each other. Hence, it is demonstrated that undersampling regularizes the source reconstruction problem by extracting the unnecessary information from the problem.

In the Section 2, the problem and its solution are described. In the Section 3, the results are presented.

2. THE DEFINITION AND THE SOLUTION OF THE PROBLEM

The $\hat{x}$ directed point source is defined as follows:

$$\vec{J}(x, y, z) = \hat{x}\; Il\; \delta(x)\, \delta(y)\, \delta(z) \tag{1}$$

with

$$Il = 1\,\mathrm{A} \cdot \mathrm{m} \tag{2}$$

Assuming a time-harmonic dependence of $e^{-j\omega t}$, the θ and ϕ components of $\vec{E}$ of the point source are given in a spherical coordinate system as follows:

$$E_\theta = \frac{je^{jkr}}{4\pi\omega\epsilon}\cos(\theta)\cos(\phi)\left(-\frac{1}{r^3}+\frac{jk}{r^2}+\frac{\omega^2\mu\epsilon}{r}\right) \tag{3}$$

$$E_\phi = -\frac{je^{jkr}}{4\pi\omega\epsilon}\sin(\phi)\left(-\frac{1}{r^3}+\frac{jk}{r^2}+\frac{\omega^2\mu\epsilon}{r}\right) \tag{4}$$

In the above equations, the symbols are defined as follows: j is the imaginary unit, ω is the angular frequency. k is the wavenumber of the medium. ϵ and μ are the permittivity and permeability of the medium respectively. r is the distance variable of the spherical coordinate system. The sampling of the electric field is carried out using these formulas.

The source to be reconstructed is expressed in terms of the Rao-Wilton-Glisson (RWG) basis functions as follows:

$$\vec{J}(\vec{r}') = \sum_{n=1}^{N} I_n \vec{f}_n(\vec{r}') \tag{5}$$

In (5), $\vec{f}_n(\vec{r}')$ is the RWG basis function [3]. $\vec{r}'$ is the distance vector of a point on the reconstruction plane. N is the number of basis functions and I_n denotes the expansion coefficients. The RWG basis function $\vec{f}_n(\vec{r}')$ is defined as follows:

$$\vec{f}_n(\vec{r}') = \begin{cases} \frac{l_n}{2A_n^+}\vec{\rho}_n^{\,+} & \text{if } \vec{r}' \text{ in } T_n^+ \\ \frac{l_n}{2A_n^-}\vec{\rho}_n^{\,-} & \text{if } \vec{r}' \text{ in } T_n^- \\ 0 & \text{if otherwise} \end{cases} \tag{6}$$

T_n^+ and T_n^- are the triangle pair belonging to the nth RWG basis function. They are shown in Fig. 1. A_n^+ and A_n^- are the areas of the triangles T_n^+ and T_n^- respectively. T_n^+ and T_n^- have one common side and two common vertices. $\vec{\rho}_n^{\,+}$ is the vector drawn from the free vertex of T_n^+ to a point in T_n^+. $\vec{\rho}_n^{\,-}$ is the vector drawn from a point in T_n^- to the free vertex of T_n^-. l_n is the length of the common edge.

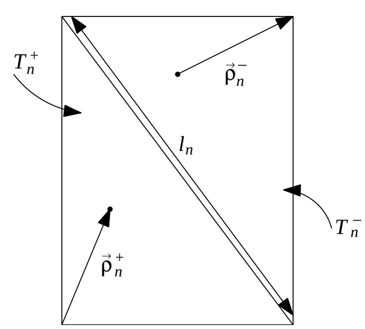

Figure 1: The triangle pair belonging to the nth RWG basis function.

Using the mixed potential integral formulation, the following integral equation is obtained for the x, y and z components of the electric field due to the nth RWG basis function:

$$E_{n_i} = \frac{j\omega\mu}{4\pi}\int_{T_n^+ + T_n^-} I_n\left[\vec{f}_n(\vec{r}')\right]_i g(\vec{r},\vec{r}')d\vec{r}' - \frac{1}{j4\pi\omega\epsilon}\frac{\partial}{\partial i}\int_{T_n^+ + T_n^-} I_n \vec{\nabla}'\cdot\vec{f}_n(\vec{r}')g(\vec{r},\vec{r}')d\vec{r}' \quad (i = x, y, z) \tag{7}$$

In (7), $g(\vec{r},\vec{r}')$ is the scalar Green's function given by:

$$g(\vec{r},\vec{r}') = \frac{e^{jk|\vec{r}-\vec{r}'|}}{|\vec{r}-\vec{r}'|} \tag{8}$$

In (8), $\vec{r}$ is the position vector of the field point. Using the integral equation in (7), the following matrix equation is obtained:

$$\begin{bmatrix}\mathbf{E}_{\boldsymbol{\theta}} \\ \mathbf{E}_{\boldsymbol{\phi}}\end{bmatrix}\mathbf{I} = \begin{bmatrix}\mathbf{b}_{\boldsymbol{\theta}} \\ \mathbf{b}_{\boldsymbol{\phi}}\end{bmatrix} \tag{9}$$

$\mathbf{E}_{\boldsymbol{\theta}}$ and $\mathbf{E}_{\boldsymbol{\phi}}$ are both $M \times N$ matrices where M is the number of sampling points on the hemisphere and N is the number of RWG basis functions. $\mathbf{E}_{\boldsymbol{\theta}}(\mathbf{p}, \mathbf{q})$ and $\mathbf{E}_{\boldsymbol{\phi}}(\mathbf{p}, \mathbf{q})$ denote the elements in the row p, column q of the matrices $\mathbf{E}_{\boldsymbol{\theta}}$ and $\mathbf{E}_{\boldsymbol{\phi}}$ respectively and are given by

$$\mathbf{E}_{\boldsymbol{\theta}}(\mathbf{p}, \mathbf{q}) = I_x^{p,q} \cos(\theta_p) \cos(\phi_p) + I_y^{p,q} \cos(\theta_p) \sin(\phi_p) - I_z^{p,q} \sin(\theta_p) \tag{10}$$

$$\mathbf{E}_{\boldsymbol{\phi}}(\mathbf{p}, \mathbf{q}) = -I_x^{p,q} \sin(\phi_p) + I_y^{p,q} \cos(\phi_p) \tag{11}$$

θ_p and ϕ_p are the θ and ϕ coordinates of the pth sampling point. The integrals I_i^{pq} $(i = x, y, z)$ are defined as

$$\begin{aligned} I_i^{pq} = & \frac{j\omega\mu}{4\pi} \int_{T_{n_q}^+} \frac{l_{n_q}}{2A_{n_q}^+} \left(\vec{\rho}_{n_q}^{\,+}\right)_i \frac{e^{jk|\vec{r}_p - \vec{r}_q'|}}{|\vec{r}_p - \vec{r}_q'|} ds' + \frac{j\omega\mu}{4\pi} \int_{T_{n_q}^-} \frac{l_{n_q}}{2A_{n_q}^-} \left(\vec{\rho}_{n_q}^{\,-}\right)_i \frac{e^{jk|\vec{r}_p - \vec{r}_q'|}}{|\vec{r}_p - \vec{r}_q'|} ds' \\ & - \frac{1}{j\omega 4\pi\epsilon} \int_{T_{n_q}^+} \frac{l_{n_q}}{A_{n_q}^+} \frac{\partial}{\partial i} \left(\frac{e^{jk|\vec{r}_p - \vec{r}_q'|}}{|\vec{r}_p - \vec{r}_q'|} \right) ds' + \frac{1}{j\omega 4\pi\epsilon} \int_{T_{n_q}^-} \frac{l_{n_q}}{A_{n_q}^-} \frac{\partial}{\partial i} \left(\frac{e^{jk|\vec{r}_p - \vec{r}_q'|}}{|\vec{r}_p - \vec{r}_q'|} \right) ds' \quad (i = x, y, z) \end{aligned} \tag{12}$$

$\vec{r}_q'$ is the position vector of a point in the triangle pair of the qth RWG basis function. $\vec{r}_p$ is the position vector of the pth sampling point. The column vector $\mathbf{I}$ in (9) is an $N \times 1$ matrix and $\mathbf{I}(q, 1)$ is the coefficient I_q used in (5). $\mathbf{b}_{\boldsymbol{\theta}}$ and $\mathbf{b}_{\boldsymbol{\phi}}$ are both $M \times 1$ matrices. $\mathbf{b}_{\boldsymbol{\theta}}(p, 1)$ and $\mathbf{b}_{\boldsymbol{\phi}}(p, 1)$ are the θ and ϕ components of the electric field respectively at the pth sampling point.

The integrals in (12) are numerically calculated using a 79 point Gaussian quadrature given in [4]. The source reconstruction problem expressed by the matrix equation is a very ill-posed problem as indicated in the first section of [5]. The matrix equation is solved by the least squares QR (LSQR) method [6]. LSQR is an effective and preferred conjugate gradient type solution method [5]. The algorithm for this method has been implemented in Fortran90 programming language by adapting the program given in [7].

If the expressions in (3) and (4) are examined, then it can be determined that the Nyquist sampling period of E_θ is $\pi^\circ \times \pi^\circ$ and of E_ϕ is π°. E_ϕ does not depend on θ.

3. THE SOURCE RECONSTRUCTION RESULTS

The operating frequency is 1 GHz. The reconstruction plane is a square of side length 0.3 m. The square is centered at the origin of the spherical coordinate system and it is in the x-z plane. The square is meshed into triangles using Siemens NX 9.0 software. The side lengths of the triangles are set to be $\lambda/\sqrt{300}$. The radius of the hemisphere on which the electric field sampling is made is 1 m. The source reconstruction problem is solved using the sampling periods of $1^\circ \times 1^\circ$, $2^\circ \times 2^\circ$, $\pi^\circ \times \pi^\circ$, $4^\circ \times 4^\circ$ and $5^\circ \times 5^\circ$ for E_θ and 1°, 2°, π°, 4° and 5° for E_ϕ. The error in the reconstructed field vector with respect to the original field vector is defined as

$$\text{error} = \sqrt{\frac{\sum_{n=1}^{M} |\text{original} - \text{reconstructed}|_n^2}{M}} \tag{13}$$

M in the summation in (13) is the number of field samples or the field vector dimension.

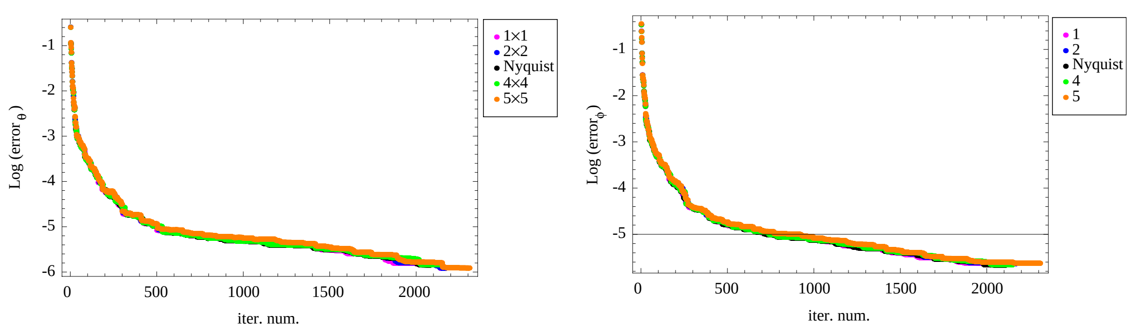

(a) (b)

Figure 2: The error in the reconstructed fields versus the LSQR iteration number. (a) The error in reconstructed E_θ. (b) The error in reconstructed E_ϕ.

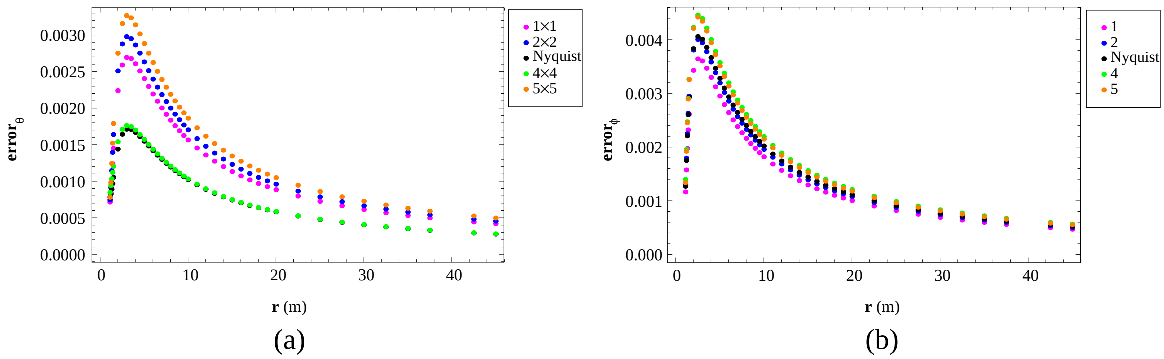

Figure 3: The plots of the error in the reconstructed field components versus the radius of the reconstruction hemisphere. (a) The error in reconstructed E_θ. (b) The error in reconstructed E_ϕ.

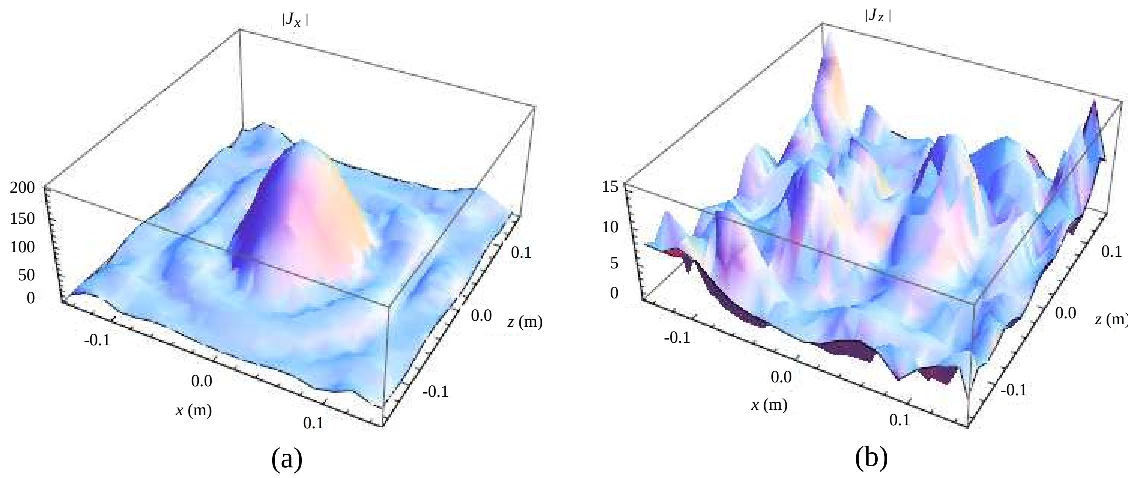

Figure 4: The magnitudes of the reconstructed electric current density components with the undersampling periods of $5^\circ \times 5^\circ$ and 5° for E_θ and E_ϕ respectively. (a) The plot of $|J_x|$. (b) The plot of $|J_z|$.

In Fig. 2, the error in the reconstructed field components are plotted versus the LSQR iteration number. As the LSQR iteration number increases, the convergence to the solution is realized. Meanwhile, the error in the reconstructed components decreases. The decrease curves are almost the same for all of the sampling rates. Hence, there is no need for oversampling or Nyquist sampling in order not to increase the computational burden in the source reconstruction problem. The oversampling and Nyquist rate sampling contains redundant information. Decreasing this redundant information by means of undersampling regularizes the problem. In Fig. 3, the reconstructed field components E_θ and E_ϕ are plotted versus the radius of the hemisphere on which the reconstruction is carried out. The error curves for various sampling rates do not differ significantly from each other. Hence, it is again proven that oversampling and Nyquist rate sampling are not necessary. Undersampling regularizes the source reconstruction problem. In Fig. 4, the spatial variations for the magnitudes of the components of the reconstructed current density are shown. This current density is reconstructed by undersampling periods of $5^\circ \times 5^\circ$ and 5° for E_θ and E_ϕ respectively. The x component can be observed to be focusing to the origin. In addition, the magnitude of the x component is at least 10 times that of the z component on the average. Hence, the reconstructed current density resembles the original x directed point source and the source reconstruction process works well.

4. CONCLUSION

A source reconstruction problem is solved for three different types of sampling schemes: Oversampling, Nyquist rate sampling and undersampling. It is demonstrated that oversampling and Nyquist rate sampling are not needed for the accurate source reconstruction. By means of undersampling, the source and field reconstruction is proven to be achieved with high accuracy. Hence, undersampling regularizes the source reconstruction problem by eliminating the redundant information due to either oversampling or Nyquist rate sampling.

ACKNOWLEDGMENT

The software NX 9.0 used for meshing has been granted by Siemens. The author has been acquainted with the source reconstruction and LSQR method during a short visit to Bilkent University Computational Electromagnetics Center (BİLCEM) and would like to thank Prof. Levent Gürel and the staff of BİLCEM.

REFERENCES

1. Las-Heras, F., M. R. Pino, S. Loredo, Y. Alvarez, and T. K. Sarkar, "Evaluating near-field radiation patterns of commercial antennas," *IEEE Trans. Antennas Propag.*, Vol. 54, 2198–2207, 2006.
2. Petre, P. and T. K. Sarkar, "Differences between modal expansion and integral equation methods for planar near-field to far-field transformation," *Progress In Electromagnetics Research*, Vol. 12, 37–56, 1996.
3. Rao, S. M., D. R. Wilton, and A. W. Glisson, "Electromagnetic scattering by surfaces of arbitrary shape," *IEEE Trans. Antennas Propag.*, Vol. 30, 409–418, 1982.
4. Dunavant, D. A., "High degree efficient symmetrical gaussian quadrature rules for the triangle," *International Journal for Numerical Methods in Engineering*, Vol. 21, 1129–1148, 1985.
5. Hansen, P. C., *Rank-deficient and Discrete Ill-posed Problems: Numerical Aspects of Linear Inversion*, SIAM, 1997.
6. Paige, C. C. and M. A. Saunders, "LSQR: An algorithm for sparse linear equations and sparse least squares," *ACM Transactions on Mathematical Software*, Vol. 8, No. 1, 43–71, 1982.
7. Saunders, M., "zlsqrmodule.f90," Jun. 29, 2013, Online Available: http://web.stanford.edu/group/SOL/software/lsqr/f90/zlsqr.zip.